Room temperature thermo-electric pumping in mid-infrared light-emitting diodes

Parthiban Santhanam,[1] Duanni Huang,[1] Rajeev J. Ram,[1] Maxim A. Remennyi,[2] and Boris A. Matveev[2]
[1]*Department of Electrical Engineering and Computer Science, Massachusetts Institute of Technology, Cambridge, Massachusetts 02139, USA*
[2]*Centre of Nanoheterostructure Physics, Ioffe Physical-Technical Institute, St. Petersburg 194021, Russia*

(Received 13 June 2013; accepted 17 October 2013; published online 1 November 2013)

We present measurements of mid-infrared light-emitting diodes generating photons above the conventional limit of 100% electrical-to-optical power conversion efficiency. At low forward bias, lattice heat is absorbed via thermo-electric effects in the carrier injection process and released radiatively through recombination, so the diode acts as a thermodynamic heat pump. Experiments support an effective temperature model for electro-luminescence in the cooling regime and refute alternative interpretations of existing results. Although non-radiative recombination limits the power density available above unity efficiency, experiments confirm the phenomenon at room temperature. © *2013 AIP Publishing LLC*. [http://dx.doi.org/10.1063/1.4828566]

The longstanding theoretical possibility[1,2] of exploiting thermo-electric heat exchange to enable light-emitting diodes (LEDs) to convert electrical power into optical power above 100% wall-plug efficiency was recently demonstrated[3] in a mid-infrared emitter at high temperature and low forward bias voltage. Here we explore this phenomenon in diodes formed from semiconductors with narrower bandgaps than in previous investigations. We present evidence of an LED operating above unity wall-plug efficiency at room temperature.

Applying a forward bias to a conventional heterojunction LED causes electrons and holes to be injected into the active region from the cathode and anode, respectively. When the electrical energy qV supplied to each electron-hole pair is less than the bandgap energy of the active region, the carriers absorb lattice heat via the Peltier effect during injection.[4–6] When these electrons and holes undergo radiative recombination, this energy is emitted as photons. When qV is less than the average energy of the photons resulting from recombination, the emitted optical power may exceed the electrical power required to drive the device. This phenomenon, known as electro-luminescent cooling, is part of a broader class of thermo-photonic effects, in which the thermodynamic entropy of the photons plays a significant role. Several modern photonic technologies already exploit photon entropy, including solid-state refrigerators based on anti-stokes laser cooling,[7,8] thermo-photo-voltaic generators,[9,10] and semiconductor diodes exhibiting negative luminescence.[11–13] The room-temperature experiments presented here address alternative interpretations of existing data and thereby provide further evidence that even conventional LEDs exhibit thermo-photonic effects. These results support the claim that conventional solid-state LEDs, independent of the material system in which they are fabricated, share the property of operating as thermodynamic heat pumps at low forward bias voltage.[3]

Design of LEDs for voltages V well below the bandgap energy E_{gap} (i.e., $E_{gap} - qV \gg k_BT$, where q is the magnitude of the electronic charge and k_BT is the ambient thermal energy) could enable devices that harness these thermo-photonic effects for improved wall-plug efficiency at higher power density. Such devices could find application as photon sources without waste heat generation,[14–16] particularly at infrared wavelengths, as well as solid-state refrigerators.[17–21] Efficient mid-infrared sources are of particular interest because the fundamental vibrational frequencies of many small molecules fall in the mid-infrared and existing sources at these wavelengths operate with limited efficiency.[22] Moreover, LEDs operating as heat pumps can become more efficient at a given power as the ambient temperature is increased. As a result, devices of this type may be particularly useful for spectroscopy in high-temperature environments such as combustion exhaust gas analysis and downhole oilfield fluid analysis.

In this work, we demonstrate room-temperature electroluminescent cooling in mid-infrared LEDs (wavelength $\lambda \approx 2$–$5\ \mu$m). At low forward bias, these LEDs act as thermodynamic heat pumps. Unlike heat engines, which utilize the natural flow of heat from hot to cold to extract work from a heat source, heat pumps do not require a temperature difference to operate. Thermodynamic heat pumps, such as the LED in this work, use externally supplied work to drive heat flow in a predetermined direction, typically from a cold reservoir to a hot reservoir. The LEDs examined here use electrical power to pump heat from their own semiconductor lattice to the outgoing optical field.

When the device is off (i.e., zero applied voltage), the lattice and the outgoing optical field are in thermal equilibrium. As the device is turned on, the outgoing photon temperature T_{photon} increases, creating a temperature difference between these modes and the lattice at ambient temperature T. In the limit of low optical output power, this temperature difference approaches zero, and the Carnot limit for efficiency of heat pumping (i.e., the heating coefficient of performance) between the reservoirs diverges. The elevated emitter temperatures from previous results are not a fundamental requirement for photon generation above unity efficiency, as demonstrated by the present work.

As with previous experiments on heated LEDs, for $qV \ll k_B T$, the applied forward bias voltage constitutes a small deviation from thermodynamic equilibrium and drives various recombination processes as a linear response. Part of this response is bimolecular recombination in the active region, which results in photon generation with an external quantum efficiency η_{EQE} that is independent of current at low bias.[3,6] Thus the current I, voltage V, and optical output power L are all linearly proportional in this regime:

$$V = I \times R_{ZB} \quad \text{and} \quad L = I \times \left(\frac{\hbar\omega}{q}\right) \times \eta_{EQE}, \tag{1}$$

where R_{ZB} is the zero-bias resistance as defined by the first equation and $\hbar\omega$ is the photon energy. The wall-plug efficiency η (or equivalently, the heating coefficient of performance) is given by the ratio of L to IV. In the low-bias regime, it is inversely proportional to output power and diverges as L approaches zero

$$\frac{L}{IV} \equiv \eta = \frac{\hbar\omega}{qV} \times \eta_{EQE} = \left(\frac{\hbar\omega}{q}\right)^2 \times \frac{\eta_{EQE}^2}{R_{ZB}} \times \frac{1}{L}. \tag{2}$$

Note that for $qV < \hbar\omega \times \eta_{EQE}$, the wall-plug efficiency exceeds unity.

From visible wavelengths to across most of the mid-infrared, the optical output power available at a fixed low-bias voltage increases as the material bandgap energy and the average energy of the emitted photons $\hbar\omega$ are reduced. For a given quantum efficiency, the increased intrinsic carrier concentration in semiconductors with smaller bandgaps leads to higher excess carrier densities at the voltage $V = (\hbar\omega/q) \times \eta_{EQE}$ where wall-plug efficiency $\eta = 1$. This increase in excess carriers leads to more photon generation and increased optical output power.

We now present a thermodynamic model to clarify the generality of the scaling of power with bandgap and ambient temperature. When a small voltage $V \ll E_{gap}/q$ is applied to a conventional LED, the electronic states near the edges of the conduction and valence band become slightly more populated with electrons and holes, respectively. This change in occupancy from equilibrium is typically characterized by introducing quasi-Fermi levels within the active region that are separated by $\Delta E_F = qV$. Alternatively, we may characterize the change in terms of the change in the effective temperature seen by inter-band processes at conditions of low forward bias, allowing us to analyze our LEDs thermodynamically and subsequently compare our experimental results with the Carnot limit. We may define the effective temperature[23] T^* as the temperature at which the product of electron and hole concentrations np with no quasi-Fermi level separation would match the value at temperature T and $\Delta E_F = qV$. For band edge states that are separated by the photon energy $\hbar\omega$, the effective temperature may be written as[23]

$$T^* = T\left(1 - \frac{qV}{\hbar\omega}\right)^{-1}, \tag{3}$$

when both species are in the dilute Boltzmann limit. More formally, T^* is the inverse of the change in entropy per unit change in energy of the combined conduction and valence band system in the thermodynamic limit when an inter-band radiative recombination or absorption event takes place.[6]

If the thickness of the LED's active region is greater than the absorption length at the emission wavelength, the net result of photon emission and reabsorption events is that each outgoing above-gap photon mode emerges occupied at the effective temperature of the electron-hole system so that $T_{photon} = T^*$. If the active region is transparent below the bandgap, the photon flux at these wavelengths may be neglected. Under these assumptions, the device glows at above-gap wavelengths with the spectral intensity of a so-called grey body[14,24] with emissivity ≈ 1 and effective temperature T^*. Simple integration then yields the following expression for the net outflow of optical power:

$$L = \int_{E_{gap}}^{\infty} d(\hbar\omega)[I(\hbar\omega; T^*) - I(\hbar\omega; T)], \tag{4}$$

where $I(\hbar\omega;T)$ is the spectral intensity of a blackbody radiator at frequency $\omega/(2\pi)$ and absolute temperature T, and T^* is a function of $\hbar\omega$. Using Eq. (3) to examine the unity efficiency operating point $V = (\hbar\omega/q) \times \eta_{EQE}$, we find

$$L_{unity} = \int_{E_{gap}}^{\infty} d(\hbar\omega)[I(\hbar\omega; T/(1 - \eta_{EQE})) - I(\hbar\omega; T)], \tag{5}$$

where L_{unity} denotes the optical power available at unity efficiency.

Because the spectral intensity of blackbody radiation near room temperature is much larger for 3.4 μm photons than for 2.15 μm photons, L_{unity} is much larger at the longer wavelength and unity wall-plug efficiency is readily observable at room temperature in these devices. At yet longer wavelengths, the increases in the spectral intensity diminish and the effects of increased leakage, non-radiative recombination, and parasitic photon reabsorption reduce low-bias η_{EQE} sufficiently that L_{unity} begins to decrease with increases in wavelength for conventional LEDs.

Equation (4) further clarifies the relationship between electro-luminescent cooling, in which a diode is operated in forward bias, and negative luminescence,[11–13] in which it is in reverse bias. In the case of negative luminescence, the reverse bias depletes an absorbing active layer so that the effective temperature of the electron-hole system for inter-band processes T^* is less than the ambient temperature T. Equation (4) again gives the cooling power, but since the heat flow has opposite sign, heat is being pumped from the photon field into the lattice. Furthermore, since the carrier density in the active region must be positive, T^* must be as well. Thus the cooling power density for negative luminescence is bounded above by the blackbody intensity at ambient temperature T, whereas there is no analogous limit for electro-luminescent cooling at forward bias.

In this work, experiments were performed on two flip-chip infrared light-emitting diodes with emission wavelengths around 3.4 and 4.7 μm. The diodes were grown by liquid-phase epitaxy on n-type InAs substrates and employed

InAs and InAsSb active regions for the 3.4 and 4.7 μm emitters, respectively.[25,26] Efficient photon extraction was achieved using a deep mesa etch, a reflective anode contact, and high-index chalcogenide adhesive to attach a hyperhemispherical Silicon lens[27] to the emitting semiconductor surface.

In previous experiments showing above-unity efficiency, the temperature of the emitter T_{LED} exceeded the temperature of the detector $T_{detector}$ by roughly 110 K. Because the measured optical power was far smaller than the net flow of blackbody radiation in the responsive band of the photo-detector, previous experiments could not fully exclude the alternative explanation that the observed optical power signal was the result of a linear modulation of the LED's emissivity.

To address this possibility, experiments near room temperature were conducted on the 3.4 μm emitter described above at low bias. To distinguish the optical signal from the blackbody background and detector noise in this regime, a 1.013 kHz square wave voltage source in series with a large resistor was used to supply about 20 pA of forward current to each device, and the optical output power was measured by zero-bias lock-in photo-detection with a 500 second time constant.

With the detector at room temperature and the emitter held slightly above and below this temperature, the photo-current signal generated by the LED in the $\eta > 1$ regime was examined. Figure 1 shows the two quadrature components of the phase-locked photo-current signal. The phase is measured relative to the drive current in the emitter. The displacement of the solid markers remains in the positive in-phase direction even as the sign of $T_{LED} - T_{detector}$ is reversed, indicating that the photo-current remains in-phase with the excitation signal.

Either a modulation of the transmission through the active region or reflection coefficient from the emitting surface would constitute a modulation of the emissivity of the LED. Since the entire apparatus on the source side was held at the same high temperature as the LED in previous experiments, transmission modulation could not be responsible for the photo-current signal observed in high-temperature experiments. By contrast, a voltage-dependent reflection coefficient could be responsible for the observations of the high-temperature experiment. If the reflection coefficient at the emitting surface R_{surf} changes inversely with voltage (i.e., $\partial R_{surf}/\partial V < 0$), during the voltage-high phase of the square wave, part of the thermal photon flux at T_{LED} would be replaced by thermal photons from surfaces facing the emitting surface. For diffuse and specular reflection, these correspond to the ambient and detector surface temperatures, respectively. When T_{LED} is higher than both the ambient and detector temperatures, the photon flux during the voltage-high phase of the excitation signal would be higher than during the voltage-low phase. Thus voltage-dependent R_{surf} could be responsible for the previous high-temperature photo-current signal.

Just as $\partial R_{surf}/\partial V < 0$ leads to an increased photon flux at positive voltage when the emitter is hot, the photon flux incident on the detector is decreased at positive voltage when T_{LED} is below the detector and ambient temperatures. Since Figure 1 shows that the photo-current in this experiment remains in phase with the excitation signal, even as T_{LED} is varied above or below the detector and ambient temperatures, voltage-dependent LED surface reflectivity is not consistent with being responsible for the observations reported here while the mechanism of thermo-electrically pumped electro-luminescent cooling of the LED is.

Next, both the 3.4 and 4.7 μm LEDs were studied across a range of operating conditions at room temperature. The results appear in Figure 2, along with previous room-temperature data[3] from a similarly-packaged 2.15 μm InGaAsSb/GaSb LED grown on a *n*-GaSb substrate.[28,29] The forward bias voltage, current, and light output were measured for each device across five orders of magnitude in current, extending from conventional operating points where the applied bias voltage qV is on the order of the bandgap energy E_{gap} down to the low-bias regime. For current levels up to

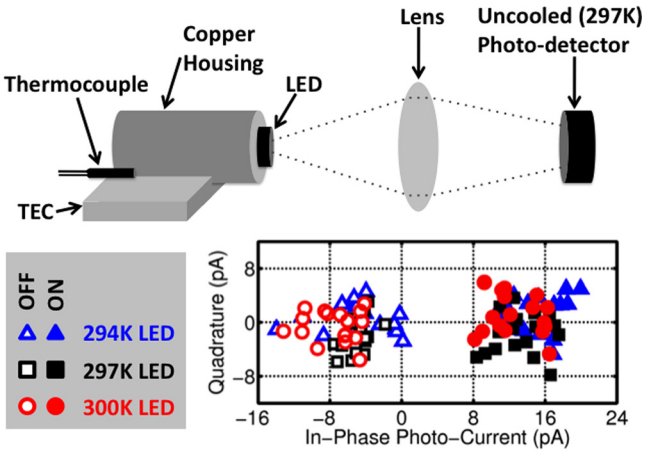

FIG. 1. At the top is a depiction of the first experiment performed on the InAs LED emitting at 3.4 μm. The thermo-electric cooler (TEC) was used to control the emitter temperature to be slightly above and slightly below the 297 K ambient. The detector was also at ambient temperature. The raw lock-in data at the bottom demonstrates that the sign of the optical power signal is independent of the sign of (T_{LED}-$T_{ambient}$) as well as (T_{LED}-$T_{detector}$) as is expected for a heat-pumping LED.

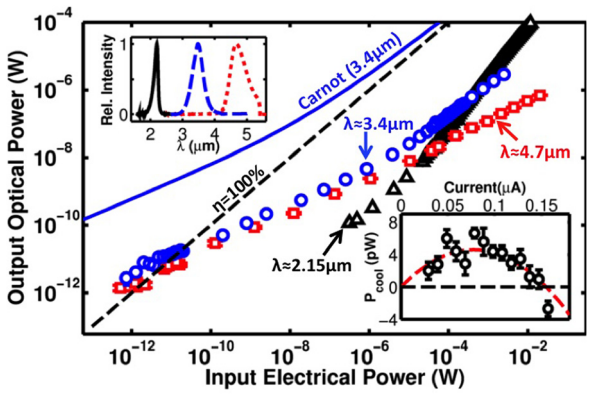

FIG. 2. Output optical power versus input electrical power for three room temperature mid-infrared LEDs. For the devices emitting at 3.4 μm (area 5.29×10^{-4} cm^2, wafer #6341) and 4.7 μm (area 2.25×10^{-4} cm^2, #236), the power at unity efficiency was high enough to be directly observed in our lock-in measurements. For the device emitting at 2.15 μm, it was not. Note: Data for the 2.15 μm LED is from Ref. 3. Insets: (top left) Relative intensity spectra for the three devices at room temperature; (bottom right) cooling power versus current for 3.4 μm device at room temperature.

2 mA, the square wave source described above was used and optical power was measured via lock-in zero-bias photo-detection with time constants as long as 500 s. For higher current measurements, a DC source-meter was used along with zero-bias DC photo-detection. DC measurements of current, voltage, and optical output power were in fair agreement with AC measurements; both types of measurements appear together in Figure 2.

For comparison, Figure 2 also includes a theoretical curve representing the Carnot limit for an emitter with the same wavelength and active area as our 3.4 μm LED. We take the idealized emitter to be optically thick at the emission wavelength, so that Eq. (4) may be used to relate a given optical power density to a temperature $T^* = T_{photon}$ above ambient. The curve represents the well-known Carnot bound $\eta < T_H/(T_H - T)$ for pumping heat from a reservoir at $T = 298$ K to a hot-side at $T_H = T_{photon}$.

For mid-infrared LEDs with a given η_{EQE}, Eq. (5) predicts that L_{unity} should increase as the photon energy decreases or the ambient temperature increases. Lock-in power measurements on the 3.4 μm LED showed that L_{unity} increased with T from 300 K up to around 420 K. Above 420 K L_{unity} decreased with T, suggesting that the increases in power at fixed voltage explained by Eqs. (3) and (4) were likely outweighed by decreases in quantum efficiency from non-radiative recombination and leakage, and the increased importance of parasitic effects from contact resistance. This temperature dependence indicates that for the 3.4 μm LED, L_{unity} is maximized when $\hbar\omega/k_BT$ is around 10. Although this does not seem to be fundamental, various authors have argued for much smaller[23] and much larger[14,30] values of $\hbar\omega/k_BT$ without experimental realization, so this phenomenological observation may serve as a guide for further experiments.

In Figure 3 we compare the results of these room-temperature power measurements with calculations based on Eqs. (3) and (4). At a fixed voltage, as the photon energy decreases, we expect that the increased effective temperature T^* of the active region electron-hole subsystem and the inclusion of modes previously below the bandgap energy will lead to increased output optical power density. For each LED, Figure 3 shows experimental data from low voltages up to half the bandgap energy. Across this range, the data is in qualitative agreement with numerical calculations. We note that the active area of the photo-diode used at 3.4 and 4.7 μm was significantly smaller (1×1mm) than that used at 2.15 μm (ø3 mm). Thus the longer-wavelength measurements may include the effect of imperfect collection efficiency by the detector; we have not corrected for this possibility in any of the data presented in this Letter.

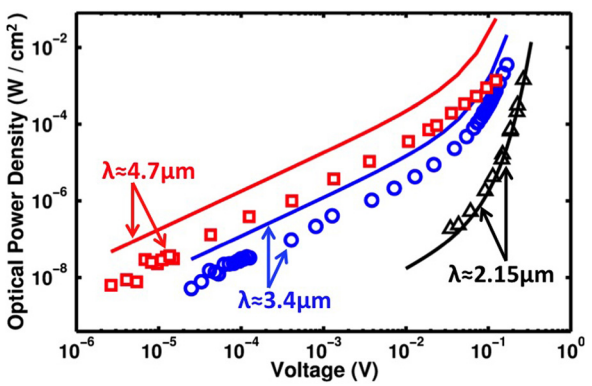

FIG. 3. Optical power density versus applied forward bias voltage for three mid-infrared LEDs. The discrete markers denote experimental data for voltages up to half the bandgap energy (i.e., $qV < E_{gap}/2$). The solid lines correspond to numerical calculations based on Eqs. (3) and (4).

At higher voltages, series resistances and other rate-limiting transport processes cause L to fall short of the calculations based on Eqs. (3) and (4). We note that our simple model must break at some voltage, since as qV approaches E_{gap} and the band-edge states approach inversion, T^* and L diverge.

In this letter we reported observations of light-emitting diodes operating above the conventional limit of 100% power conversion efficiency at room temperature. We examined multiple mid-infrared LEDs fabricated in different material systems and emitting at different wavelengths. We find that for voltages well below the bandgap energy, the power density of heat pumping is well described by an effective temperature radiation model.

We thank N.M. Stus' (Ioffe Institute) for assistance in the study.

[1]J. Tauc, Czech. J. Phys. **7**, 275–276 (1957).
[2]M. A. Weinstein, J. Opt. Soc. Am. **50**(6), 597–602 (1960).
[3]P. Santhanam, D. J. Gray, Jr., and R. J. Ram, Phys. Rev. Lett. **108**, 097403 (2012).
[4]K. P. Pipe, R. J. Ram, and A. Shakouri, Phys. Rev. B **66**, 125316 (2002).
[5]S.-Q. Yu, J.-B. Wang, D. Ding, S. R. Johnson, D. Vasileska, and Y.-H. Zhang, "Light-emitting diodes: Research, manufacturing, and applications XI," Proc. SPIE **6486**, 648604 (2007).
[6]P. Santhanam, D. Huang, D. J. Gray, Jr., and R. J. Ram, "Laser refrigeration of solids VI," Proc. SPIE **8638**, 863807 (2013).
[7]R. I. Epstein, M. I. Buchwald, B. C. Edwards, T. R. Gosnell, and C. E. Mungan, Nature **377**, 500–503 (1995).
[8]D. V. Seletskiy, S. D. Melgaard, S. Bigotta, A. D. Lieto, M. Tonelli, and M. Sheik-Bahae, Nature Photon. **4**, 161–164 (2010).
[9]T. J. Coutts and M. C. Fitzgerald, Sci. Am. **279**(3), 90–95 (1998).
[10]N.-P. Harder, D. H. Neuhaus, P. Würfel, A. G. Aberle, and M. A. Green, in *Proceedings of 17th European Photo-Voltaic Solar Energy Conference* (WIP-Munich, Germany, 2001), pp. 102–106.
[11]V. I. Ivanov-Omskii, B. T. Kolomiets, and V. A. Smirnov, Sov. Phys. Dokl. **10**, 345–346 (1965).
[12]V. I. Ivanov-Omskii and B. A. Matveev, Semiconductors **41**(3), 247–258 (2007).
[13]W. W. Bewley, J. R. Lindle, I. Vurgaftman, J. R. Meyer, J. L. Johnson, M. L. Thomas, and W. E. Tennant, Appl. Phys. Lett. **83**(16), 3254–3256 (2003).
[14]O. Heikkilä, J. Oksanen, and J. Tulkki, J. Appl. Phys. **105**, 093119 (2009).
[15]O. Heikkilä, J. Oksanen, and J. Tulkki, J. Appl. Phys. **107**, 033105 (2010).
[16]L. Yang and X. Yan, *Solid State Lighting Reliability* (Springer, 2013), pp. 497–556.
[17]P. Han, K.-J. Jin, S.-F. Ren, Y.-L. Zhou, and H.-B. Lu, J. Appl. Phys. **102**, 114501 (2007).
[18]S.-T. Yen and K.-C. Lee, J. Appl. Phys. **107**, 054513 (2010).
[19]J.-B. Wang, S. R. Johnson, D. Ding, S.-Q. Yu, and Y.-H. Zhang, J. Appl. Phys. **100**, 043502 (2006).
[20]R. Kascha, German patent application DE202,007,010,981U1 (2007).
[21]A. G. Mal'shukov and K. A. Chao, Phys. Rev. Lett. **86**(24), 5570–5573 (2001).
[22]G. Y. Sotnikova, G. A. Gavrilov, S. E. Aleksandrov, A. A. Kapralov, S. A. Karandashev, B. A. Matveev, and M. A. Remennyi, IEEE Sens. J. **10**(2), 225–234 (2010).
[23]P. Berdahl, J. Appl. Phys. **58**(3), 1369–1374 (1985).
[24]P. Würfel, J. Phys. C **15**, 3967–3985 (1982).

[25]B. A. Matveev, N. V. Zotova, N. D. Il'inskaya, S. A. Karandashev, M. A. Remennyi, N. M. Stus', A. P. Kovchavtsev, G. L. Kuryshev, and V. G. Plovinkin, in "Progress in Semiconductor Materials V—Novel Materials and Electronic and Optoelectronic Applications" (Mater. Res. Soc. Symp. Proc., 2006), Vol. 891-EE01-04, pp. 1–6.
[26]B. A. Matveev, M. Aydaraliev, N. V. Zotova, S. A. Karandashev, M. A. Remennyi, N. M. Stus, G. N. Talalakin, V. K. Malyutenko, and O. Y. Malyutenko, "Testing, reliability, and applications of optoelectronic devices," Proc. SPIE **4285**, 109–117 (2001).
[27]S. A. Karandashev, B. A. Matveev, M. A. Remennyi, A. A. Shlenskii, L. S. Lunin, V. I. Ratushnyi, A. V. Koryuk, and N. G. Tarakanova, Semiconductors **41**(11), 1369–1374 (2007).
[28]N. V. Zotova, N. D. Il'inskaya, S. A. Karandashev, B. A. Matveev, M. A. Remennyi, N. M. Stus', and A. A. Shlenskii, Semiconductors **40**(3), 351–356 (2006).
[29]Data sheet for Ioffe LED, Ltd. Model LED21Sr.
[30]G. C. Dousmanis, C. M. Mueller, H. Nelson, and K. G. Petzinger, Phys. Rev. **133**(1A), A316–A318 (1964).